Fire-induced albedo change and its radiative forcing at the surface in northern Australia

Y. Jin[1,2] and D. P. Roy[1,3]

Received 24 February 2005; revised 9 May 2005; accepted 26 May 2005; published 1 July 2005.

[1] This paper investigates the impact of fire on surface albedo and the associated radiative forcing over 56% of continental Australia encompassing the fire-prone northern tropical savanna. Fire-affected areas and albedos are derived for the 2003 fire season using daily Moderate Resolution Imaging Spectroradiometer (MODIS) surface reflectance data. Near-infrared and total shortwave albedos are observed to generally decrease after fire occurrence. Regionally, the total shortwave albedo drops by an average of 0.024, with increasing reductions as the dry season progresses and larger reductions in grasslands than woody savannas. These fire-induced albedo changes exert a positive forcing at the surface that increases from March to November. A mean "instantaneous" shortwave surface radiative forcing of 0.52 Wm^{-2} is estimated for the study region. **Citation:** Jin, Y., and D. P. Roy (2005), Fire-induced albedo change and its radiative forcing at the surface in northern Australia, *Geophys. Res. Lett.*, *32*, L13401, doi:10.1029/2005GL022822.

1. Introduction

[2] Surface albedo affects the Earth's radiative energy balance, by controlling how much incoming solar radiation is absorbed by the surface. It is well established that land use changes that affect physical surface properties including albedo impose a radiative forcing on the climate [*Intergovernmental Panel on Climate Change* (*IPCC*), 2001]. Confidence in albedo-related radiative forcing estimates remain low due to several factors, including the small number of investigations and uncertainties in the land cover change and the albedo data sets used to drive them [*IPCC*, 2001]. Most studies have concentrated on anthropogenic land use/cover changes which generally lead to increased albedo and negative radiative forcing [*Betts*, 2001; *Myhre and Myhre*, 2003]. Human-induced albedo changes are estimated to have caused a mean global radiative forcing of -0.2 Wm^{-2} since the pre-industrial period and may be comparable with forcings due to anthropogenic aerosols, solar variation, and greenhouse gases [*Hansen et al.*, 1998].

[3] Fire is a major cause of surface change and occurs in most vegetation zones across the world. Fire destroys vegetation and deposits charcoal and ash, which generally reduces reflectance, especially at infrared wavelengths [*Roy et al.*, 2005]. *Govaerts et al.* [2002] analyzed a Meteosat temporal surface albedo data set over Northern Hemisphere Africa and estimated that fires cause a relative albedo decrease of up to 25%. The effect of fire on albedo is complex and depends on the pre-fire vegetation structure and underlying soil reflectance; the combustion completeness of the fire; unburned leaf drop; and vegetation regrowth and recovery after the fire [*Roy and Landmann*, 2005]. Fire-induced albedo changes and their impact on the radiation balance have not been comprehensively investigated, especially at regional and continental scale, in contrast to numerous studies on the radiative impact of greenhouse gases and aerosols emitted from biomass burning [*IPCC*, 2001].

[4] This study aims to quantify the albedo change due to fire and the associated shortwave radiative forcing at the surface under typical incoming solar radiation. To decouple the forcings contributed by albedo and aerosol changes, we do not explicitly consider the impact of biomass burning aerosols on incoming radiation [*Christopher et al.*, 2000]. Rather than using imprecise inventory data, we derive fire-affected areas and pre- and post-fire albedos in a spatially and temporally explicit manner using satellite data. We restrict our study to the predominant 2003 fire season of Australia north of 26.5°S, an area equivalent to 56% of continental Australia, encompassing the tropical savanna. The monsoon-driven wet November–April summers and dry May–October winters produce moderate to severe fire weather and accumulated dry fuels which result in a high frequency of fires [*Bradstock et al.*, 2002]. Recent continental-scale mapping using NOAA-AVHRR satellite data for 1997 to 2001 has shown that the greatest extent of Australian fire occurs in the tropical savanna, where an average of 19% of the area burned annually (with annual means varying from 13% to 27%) [*Russell-Smith et al.*, 2003]. Global sensitivity analysis performed by increasing albedo by 0.01 indicates more significant forcing in this and other tropical regions than at mid- and high latitudes [*Myhre and Myhre*, 2003].

2. Data and Methods

[5] We map fire-affected areas and quantify surface albedo changes using time series of daily atmospherically corrected surface reflectance at 500 m resolution acquired from the MODIS instruments aboard the NASA Terra (morning overpass) and Aqua (afternoon overpass) polar orbiting satellites [*Vermote et al.*, 2002]. MODIS has seven reflective bands for land studies, from the visible to middle infrared wavelengths. We reject all observations with cloud,

[1]Department of Geography, University of Maryland, College Park, Maryland, USA.
[2]Now at Department of Earth System Science, University of California, Irvine, California, USA.
[3]Also at NASA Goddard Space Flight Center, Greenbelt, Maryland, USA.

0094-8276/05/2005GL022822$05.00

snow, bad quality, high solar or view zenith angle (>65°) [*Roy et al.*, 2005]. Recently processed (Collection 4) 2003 MODIS data are used.

[6] The location and approximate day of burning is mapped using a change detection approach applied to the MODIS near-infrared and shortwave infrared bands [*Roy et al.*, 2005]. The RossThick-LiSparse reciprocal (RTLSR) Bi-directional Reflectance Distribution Function (BRDF) model [*Schaaf et al.*, 2002] is inverted against 7 or more surface directional reflectances observed within 16 to 32 days. Model prediction at subsequent observation sun-view geometries provides an expectation and uncertainty of their reflectance. A statistical measure is used to determine if the difference between the predicted and observed reflectance is significant. Spectral constraints defined by the noise characteristics of the reflectance data and knowledge of the spectral behavior of burned vegetation are used to reject non-fire related changes. By moving through the time series, temporal constraints capitalizing on the spectral persistence of fire-affected areas are applied, and the day of burning derived. The fire-affected areas are generated here by combined use of the daily MODIS Aqua and Terra observations which provides improved detection over using one of these data streams alone.

[7] Surface albedos and their uncertainties are derived independently before and after the date of burning using a modified MODIS albedo product approach [*Schaaf et al.*, 2002]. The RTLSR BRDF model is inverted against 7 or more directional surface reflectance observations sensed within a temporal window of 16 days. The temporal window is expanded as necessary until there are 7 observations, up to a maximum window duration of 32 days. The white-sky albedo (diffuse illumination) is then derived for each of the seven spectral bands by integrating the retrieved BRDF over the illuminating and reflecting hemispheres [*Wang et al.*, 2004]. The spectral albedos are converted to broadband albedos in the visible (0.3–0.7 μm), near-infrared (0.7–5.0 μm) and total shortwave (0.3–5.0 μm). The albedo uncertainty is quantified as the product of the noise magnification factor and the root mean square error of the BRDF inversion [*Lucht and Lewis*, 2000]. Both the daily MODIS Terra and Aqua observations are used for more reliable albedo estimates [*Lucht and Lewis*, 2000].

[8] For each fire-affected 500 m pixel, the shortwave radiative forcing at the surface ($\Delta F_{surface}$) contributed by fire-induced albedo change only is estimated as:

$$\Delta F_{surface} = -I^{\downarrow}_{surface} \cdot (\alpha_2 - \alpha_1) \quad (1)$$

where $I^{\downarrow}_{surface}$ is the surface incoming solar radiation [Wm^{-2}] and ($\alpha_2 - \alpha_1$) is the "instantaneous" surface albedo change computed by subtracting the pre-fire albedo (α_1) from the post-fire albedo (α_2). The European Centre for Medium-Range Weather Forecasts 40-year Reanalysis (ERA40) provides monthly mean surface incoming solar radiation at 2.5° by 2.5° grid cells from September 1957 to August 2002 [*Allan et al.*, 2004]. To derive climatology of incoming solar radiation $I^{\downarrow}_{surface}$, we calculate ERA40 multi-year monthly means from January 1979 onward. The MODIS 1 km land cover product [*Friedl et al.*, 2002] is also used to examine differences among IGBP land cover types.

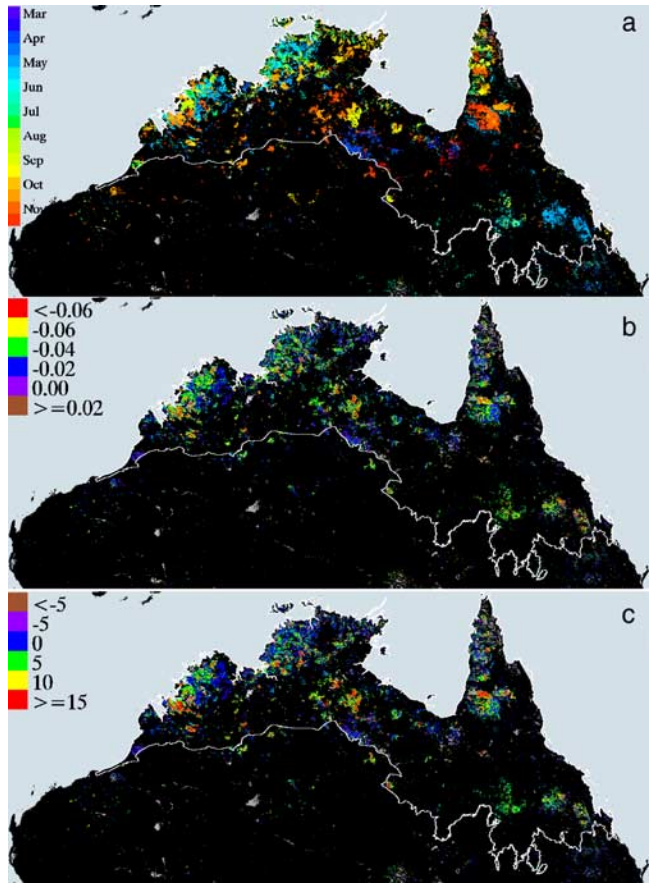

Figure 1. Spatial distribution of (a) fire affected areas and approximate day of burning (colors) in 2003; (b) "instantaneous" albedo change; (c) surface radiative forcing [Wm^{-2}] in the total shortwave, for Australia north of 26.5°S (in Lambert Azimuthal projection). Light grey indicates locations with insufficient data to produce results. The white vector illustrates the extent of the Australian Tropical Savanna.

3. Results

[9] Figure 1a illustrates the study region and the fire-affected areas detected by MODIS for March to November 2003. The total area burned is 422,640 km^2, corresponding to 8.4% of the total land area (5,022,690 km^2). Most fires occurred north of 20°S, where 18% (352,450 km^2) of the land was burned. The most extensive burned areas were in the Kimberley Plateau, Western Australia, the Top End/Gulf of Carpentaria in Northern Territory, and The Cape York Peninsula in Queensland. By IGBP land cover types, most burning occurred in the savannas (134,740 km^2), woody savannas (122,160 km^2), open shrublands (66,700 km^2), and grasslands (54,570 km^2). Fires occurred in all of the dry season, mainly from August onwards. Figures 1b and 1c show the "instantaneous" shortwave albedo change and the radiative forcing at the surface for all of the burned pixels (Figure 1a). It is apparent that fire leads to a general decrease of albedo and a positive surface radiative forcing.

[10] The albedo change caused by fire varies both spectrally and seasonally. Figure 2 illustrates mean pre-fire and post-fire albedo values derived for Queensland savanna pixels only to reduce geographic variations in vegetation and fire behavior. The error bars depict the mean albedo uncertainties. For those pixels burned in November, Figure 2a shows the mean pre-fire and post-fire albedos over the seven MODIS reflective bands and three broadbands. Fire reduces the mean albedo in all reflective bands, except the 0.4690 μm (blue) and 2.130 μm (middle infrared) bands. The greatest drop in albedo is found in the 0.858 μm and 1.240 μm near infrared bands, which is due to the high contrast between the reflectivity of vegetation and charcoal at these wavelengths. The magnitude of albedo decrease for the 0.555 μm (green), 0.645 μm (red) and 1.640 μm (middle infrared) bands are small compared to their uncertainties. These spectral characteristics of albedo change are consistent with field radiometry and satellite observations [*Trigg and Flasse*, 2000; *Roy et al.*, 2005]. The broadband albedos decrease by 14% from 0.182 to 0.156 in the total shortwave, by 13% from 0.261 to 0.226 in the near infrared, and slightly by 4% from 0.083 to 0.079 in the visible. The uncertainty of the albedo retrieval generally increases after fire occurrence, e.g., the mean shortwave uncertainty increases from 0.010 to 0.016. This increased uncertainty is caused by post-fire changes in surface reflectivity primarily associated with dissipation of charcoal and ash and vegetation regrowth [*Bradstock et al.*, 2002] over the 16 to 32 day period used to calculate post-fire albedo.

[11] Figure 2b shows the pre-fire and post-fire broadband albedos for Queensland savanna pixels that burned within each month. The pre-fire near-infrared and shortwave albedo values exhibit a seasonal trend consistent with the vegetation phenology i.e., senescence and greenup before and after the southern hemisphere winter in July–August. The corresponding post-fire albedo values follow a similar trend but have consistently lower values. The reduction in broadband albedo is greatest in the late dry season. This is likely because of the drier fuel loads and the hot weather that cause fires to burn more completely [*Williams et al.*, 1998]. When averaged over the study region by each land cover type, the shortwave albedo decreases by 0.009, 0.023,

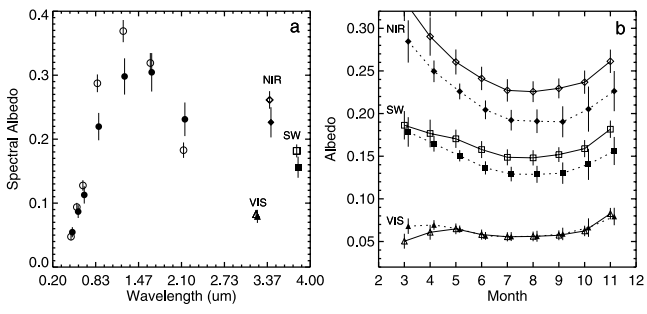

Figure 2. The spectral and temporal dependence of surface albedo before fire (open symbols) and after fire (filled symbols) for burned savanna pixels in Queensland: (a) Mean albedos in November for seven MODIS land bands (circles) plotted at the band center, and for the broadband visible, near-infrared and shortwave; (b) mean monthly pre- and post-fire broadband albedos. The mean albedo uncertainties are plotted as vertical bars.

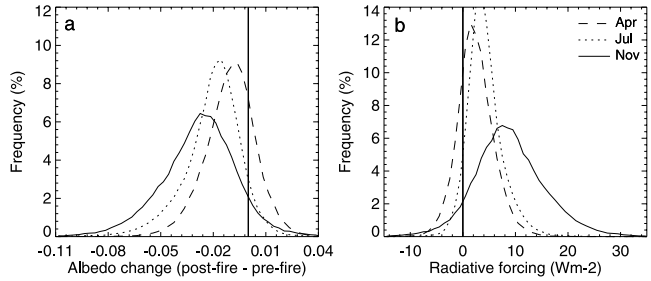

Figure 3. Frequency distribution of total shortwave (a) albedo change; (b) surface radiative forcing. Results are shown for all land pixels burned over the study area in April (dashed), July (dotted), and November (solid). Vertical zero-value lines are superimposed for reference.

and 0.035 for grassland fires occurring in April, July, and November, respectively; by 0.011, 0.021, and 0.030 over savannas; by 0.010, 0.019, and 0.025 over open shrublands; and, by 0.014, 0.021, and 0.024 over woody savannas. These differences among land covers are likely related to differences in fuel composition and combustion characteristics, with generally higher combustion completeness observed in grasslands than woodlands [*Hoffa et al.*, 1999].

[12] Figure 3 shows histograms of the shortwave albedo change and the surface radiative forcing for all land pixels burned in April (end of wet season), July (early dry season) and November (late dry season), respectively. These data are approximately normally distributed. The change in shortwave albedo is greatest in November with a mean change of −0.028 (relative −15%) and a standard deviation of 0.022. The November forcing has a mean of 8.93 Wm^{-2} and a standard deviation of 6.84 Wm^{-2}. Similar results are observed for April and July but the magnitudes and variations of the changes are smaller, due to differences in the geographic distribution of the fire-affected areas in these months and perhaps less complete burning in the early dry season [*Williams et al.*, 1998; *Hoffa et al.*, 1999]. In all months only a small proportion of burned pixels exhibit an increase in shortwave albedo and a negative forcing. We hypothesize that these are associated with vegetation removal by fire to expose relatively drier and brighter underlying soils in the visible spectrum.

[13] Figure 4 summarizes for the months March to November and over the detected burned areas the mean of the surface incoming solar radiation, the "instantaneous" shortwave albedo change due to fire, and the shortwave surface radiative forcing. The vertical bars illustrate the spatial variations (standard deviation) of these values. Overall, the magnitude of albedo change increases from the early dry season to the late dry season, from winter to spring, for the reasons discussed earlier. The forcing over the burned areas has an increasing trend from March (mean 1.78 Wm^{-2}) to November (mean 8.93 Wm^{-2}). This is despite the decreasing incoming solar radiation before July (minimum in June) which is counteracted by the increasing magnitude of albedo change in this period.

[14] Finally, by considering the temporally and spatially explicit results shown in Figure 1 we estimate a mean 2003 regional "instantaneous" shortwave albedo change of −0.024 ($1\sigma = 0.019$) over all the burned areas in the study region. This albedo change exerts a mean "instantaneous"

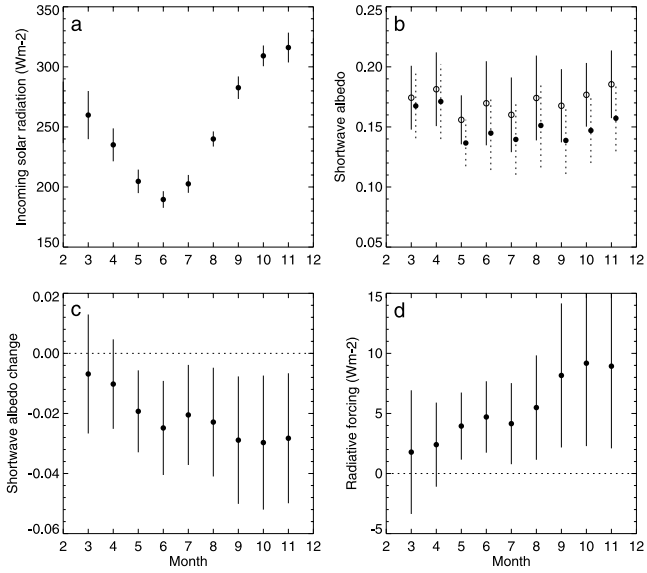

Figure 4. Temporal change of (a) mean monthly ERA40 climatology incoming solar radiation at the surface; (b) mean pre-fire (open circles) and post-fire (filled circles) shortwave albedos; (c) albedo change; and (d) surface shortwave radiative forcing over all burned areas. The spatial variations (one standard deviation) are plotted as vertical bars. Horizontal dashed zero-value lines are plotted for reference.

shortwave surface radiative forcing over the burned areas of 6.23 Wm^{-2} (spatial variation: $1\sigma = 6.08$). Multiplying this forcing with the proportion of the total area burned to the total land area gives a mean regional surface forcing of 0.52 Wm^{-2} ($1\sigma = 0.53$). Similarly, considering all the land north of 20°S, where the majority of fires occur, gives a mean surface forcing of 1.18 Wm^{-2} ($1\sigma = 1.20$).

4. Summary and Discussions

[15] Regional forcing studies have been recommended for a better understanding of climate response to land use/cover changes [*National Research Council*, 2005]. This regional study quantifies the ''instantaneous'' albedo change within 16 to 32 days after fire and the associated shortwave surface radiative forcing for Australia north of 26.5°S. In 2003 the total shortwave albedo decreased by an average of 0.024 over a burned area of 422,640 km^2. The albedo decreased by a greater amount in grasslands than woody savannas and as the dry season progressed. These fire-induced albedo changes resulted in a positive surface shortwave radiative forcing, estimated as 6.23 Wm^{-2} on average over the burned areas and as 0.52 Wm^{-2} over the study region. Our analysis reveals an increasing trend of forcing from March to November, indicating that the overall forcing will be reduced if more burning occurs in the early dry season for the same annual area burned.

[16] Long-term studies of the temporal evolution of fire-induced albedo change are needed to derive annual mean regional forcing estimates. These studies should consider forcing over several years to capture interannual variability in the seasonality of burning and the annual area burned. Our analysis did not explicitly consider the impact of biomass burning aerosols on incoming solar radiation, although aerosol climatology was used in the ERA40 reanalysis [*Allan et al.*, 2004]. The aerosols from biomass burning often cause a negative forcing [*Christopher et al.*, 2000], which may counteract the positive forcing due to albedo decreases. For a complete account of forcing from fire, further research is needed to consider both albedo and aerosol effects.

[17] **Acknowledgments.** This work was funded by the NASA Earth System Science (grant NNG04HZ18C) and Land Cover and Land Use Change and Applications (NAG511251) programs. The Tropical Savannas Cooperative Research Centre, Australia provided the Tropical Savanna vector data. The reviewers are thanked for their constructive comments.

References

Allan, R. P., M. A. Ringer, J. A. Pamment, and A. Slingo (2004), Simulation of the Earth's radiation budget by the European Centre for Medium-Range Weather Forecasts 40-year reanalysis (ERA40), *J. Geophys. Res.*, *109*, D18107, doi:10.1029/2004JD004816.

Betts, R. (2001), Biogeophysical impacts of land use on present-day climate: Near-surface temperature and radiative forcing, *Atmos. Sci. Lett.*, *1*, doi:10.1006/asle.2000.0023.

Bradstock, R. A., et al. (2002), *Flammable Australia: The Fire Regimes and Biodiversity of a Continent*, Cambridge Univ. Press, New York.

Christopher, S. A., J. Chou, J. Zhang, X. Li, T. A. Berendes, and R. M. Welch (2000), Shortwave direct radiative forcing of biomass burning aerosols estimated from VIRS and CERES, *Geophys. Res. Lett.*, *27*, 2197–2200.

Friedl, M. A., et al. (2002), Global land cover from MODIS: Algorithms and early results, *Remote Sens. Environ.*, *83*, 287–302.

Govaerts, Y. M., J. M. Pereira, B. Pinty, and B. Mota (2002), Impact of fires on surface albedo dynamics over the African continent, *J. Geophys. Res.*, *107*(D22), 4629, doi:10.1029/2002JD002388.

Hansen, J., et al. (1998), Climate forcings in the Industrial Era, *Proc. Natl. Acad. Sci.*, *95*, 12,753–12,758.

Hoffa, E. A., et al. (1999), Seasonality of carbon emissions from biomass burning in a Zambian savanna, *J. Geophys. Res.*, *104*, 13,841–13,853.

Intergovernmental Panel on Climate Change (IPCC) (2001), *Climate Change 2001: The Scientific Basis: Contribution of Working Group I to the Third Assessment Report of the Intergovernmental Panel on Climate Change*, edited by J. T. Houghton et al., 881 pp., Cambridge Univ. Press, New York.

Lucht, W., and P. Lewis (2000), Theoretical noise sensitivity of BRDF and albedo retrieval from the EOS-MODIS and MISR sensors with respect to angular sampling, *Int. J. Remote Sens.*, *21*, 81–98.

Myhre, G., and A. Myhre (2003), Uncertainties in radiative forcing due to surface albedo changes caused by land-use changes, *J. Clim.*, *16*, 1511–1524.

National Research Council (2005), *Radiative Forcing of Climate Change: Expanding the Concept and Addressing Uncertainties*, 92 pp., Natl. Acad. Press, Washington, D. C.

Roy, D. P., and T. Landmann (2005), Characterizing the surface heterogeneity of fire effects using multi-temporal reflective wavelength data, *Int. J. Remote Sens.*, in press.

Roy, D. P., et al. (2005), Prototyping a global algorithm for systematic fire-affected area mapping using MODIS time series data, *Remote Sens. Environ.*, in press.

Russell-Smith, J., et al. (2003), Contemporary fire regimes of northern Australia, 1997–2001: Changes since Aboriginal occupancy, challenges for sustainable management, *Int. J. Wildland Fire*, *12*, 283–297.

Schaaf, C., et al. (2002), First operational BRDF, albedo and nadir reflectance products from MODIS, *Remote Sens. Environ.*, *83*, 135–148.

Trigg, S., and S. Flasse (2000), Characterizing the spectral-temporal response of burned savannah using in situ spectroradiometry and infrared thermometry, *Int. J. Remote Sens.*, *21*, 3161–3168.

Vermote, E. F., et al. (2002), Atmospheric correction of MODIS data in the visible to middle infrared: First results, *Remote Sens. Environ.*, *83*, 97–111.

Wang, Z., et al. (2004), Using MODIS BRDF and albedo data to evaluate global model land surface albedo, *J. Hydrometeorology*, *5*, 3–14.

Williams, R. J., et al. (1998), Seasonal changes in fire behavior in a tropical savanna in northern Australia, *Int. J. Wildland Fire*, *8*, 227–239.

Y. Jin and D. P. Roy, Department of Geography, University of Maryland, College Park, MD 20742, USA. (yufang@uci.edu)